



Applied
Remote Sensing
and Analysis

NOVEMBER 30, 2012



Kaibab National Forest

Technical Data Report

LiDAR Delivery 2



Bret Hazell
3Di West
3400 W. 11th Avenue
Eugene, OR 97402
Ph: 541-343-8877



WSI Corvallis Office
517 SW 2nd St., Suite 400
Corvallis, OR 97333
PH: 541-752-1204

TABLE OF CONTENTS

| | |
|----------------------------------|----|
| INTRODUCTION | 1 |
| ACQUISITION..... | 4 |
| Planning | 4 |
| Ground Survey | 5 |
| Monumentation..... | 5 |
| RTK | 7 |
| Airborne Survey..... | 9 |
| LiDAR..... | 9 |
| PROCESSING | 11 |
| LiDAR Data | 11 |
| RESULTS & DISCUSSION | 13 |
| LiDAR Density | 13 |
| LiDAR Accuracy Assessments | 19 |
| LiDAR Absolute Accuracy | 19 |
| LiDAR Relative Accuracy | 20 |
| SELECTED IMAGES | 21 |
| GLOSSARY..... | 25 |
| APPENDIX A..... | 26 |
| APPENDIX B..... | 27 |

Cover Photo: View looking north at Cape Final of the Walhalla Plateau in Kaibab National Forest, AZ. Image derived from gridded LiDAR points colored by 2010 NAIP imagery.

INTRODUCTION

3D point cloud looking at the Kaibab National Forest site in Arizona



In August 2012, WSI (Watershed Sciences, Inc.) was contracted by 3Di West to collect Light Detection and Ranging (LiDAR) data in the fall of 2012 for the Kaibab National Forest/Grand Canyon National Park site in Arizona (Figure 1). Data were collected to aid 3Di West and the USDA Forest Service in assessing the site for Northern Goshawk habitat properties.

The following report accompanies the delivered LiDAR data, documenting the data acquisition, processing methods, and accuracy assessments. Project extent and timeline for contracted data products are provided below (Table 1) including contracted deliverables provided to 3Di West (Table 2).

Table 1: Acquisition dates, acreages, and data types collected on the Kaibab National Forest

| Delivery Schedule | Delivery Date | Contracted Acres | Buffered Acres | Acquisition Dates | Data Type |
|-------------------|---------------|------------------|----------------|--|-----------|
| Delivery 1 | 10/31/2012 | 108,745 | 109,871 | Aug. 25-31,2012 Sept. 1,3-9,13-15, 2012 | LiDAR |
| Delivery 2 | 11/30/2012 | 336,582 | 348,054 | | |

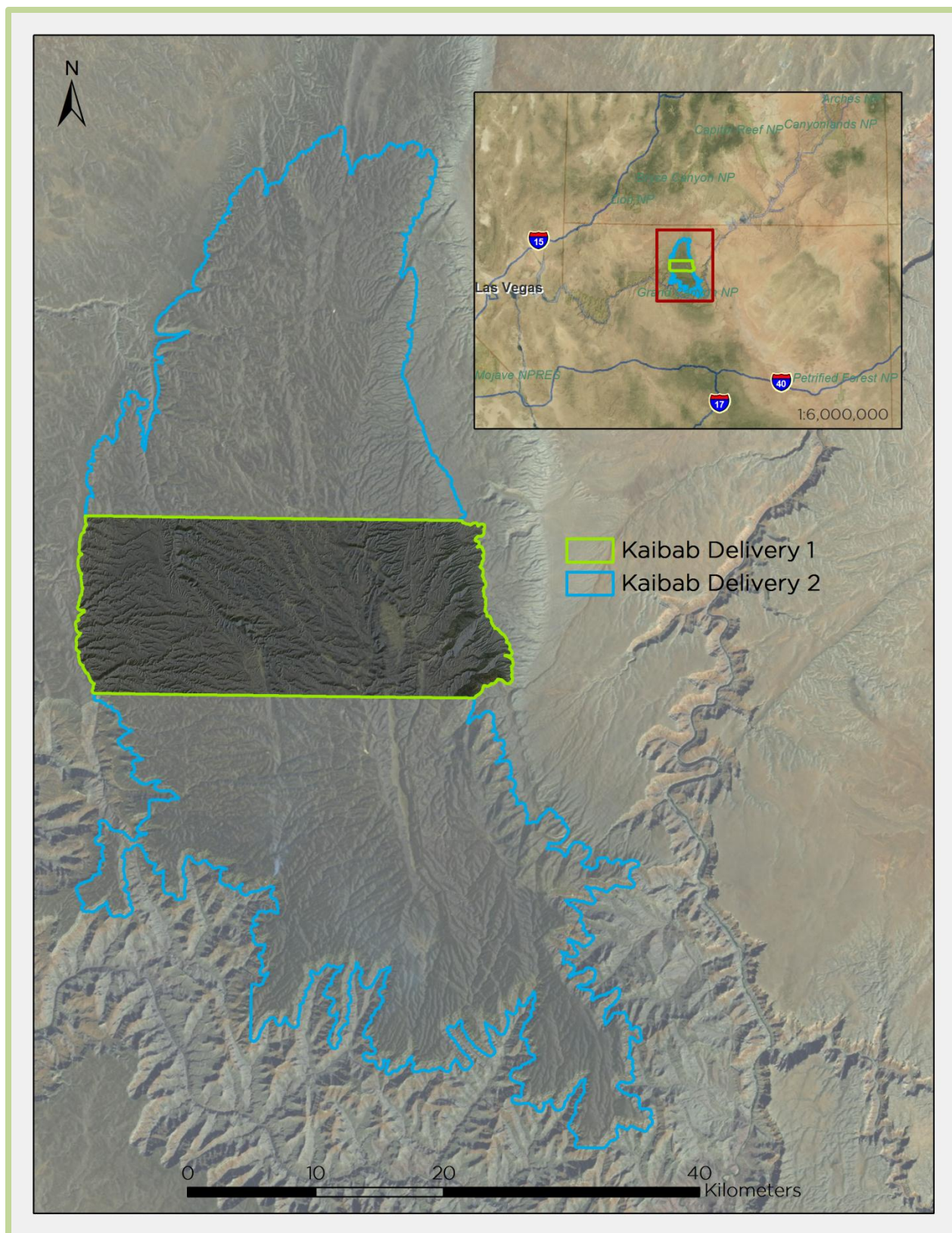


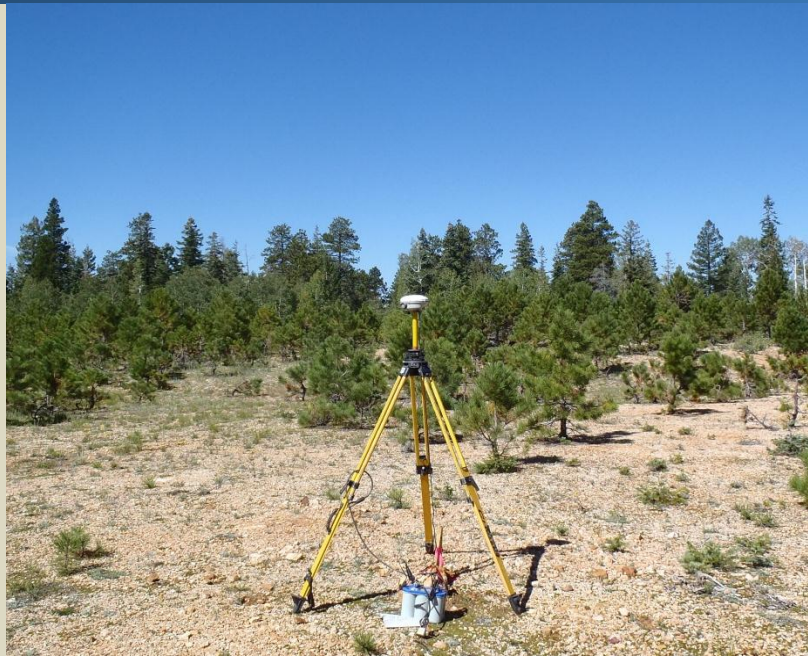
Figure 1: Location map of the Kaibab National Forest LiDAR acquisition

Table 2: Products delivered to 3Di West for Delivery 2 of the Kaibab National Forest LiDAR project

| Kaibab National Forest Products Projection: UTM Zone 12 North Horizontal Datum: NAD83 (HARN) Vertical Datum: NAVD88 (GEOID03) Units: Meters | |
|--|--|
| LAS Files | LAS v 1.2 <ul style="list-style-type: none"> • All Returns • Ground Returns |
| Rasters | 1 Meter ESRI Grids and GeoTiffs <ul style="list-style-type: none"> • Bare Earth Model • Highest Hit Model 0.5 Meter GeoTiffs <ul style="list-style-type: none"> • Intensity Images |
| Vectors | Shapefiles (.shp) <ul style="list-style-type: none"> • Site Boundary • LiDAR Index • DEM/DSM Index • Flightlines/Swaths • Smooth Best Estimate Trajectory (SBETs) Geodatabases (*.gdb) <ul style="list-style-type: none"> • Ground Point feature classes |



Trimble R8 survey setup at the Kaibab National Forest site



Planning

In preparation for data collection, WSI reviewed the project area using Google Earth, and flightlines were developed using ALTM-NAV Planner (v.3.0) software. Careful planning entailed adapting the pulse rate, flight altitude and ground speed to ensure complete coverage (no gaps) of the Kaibab National Forest study area at the requested pulse density of ≥ 8 pulses per square meter while optimizing flight paths to minimize flight times.

This process entails preparing for known factors such as satellite constellation availability and weather windows. In addition, a variety of logistical considerations require review: private property access, potential air space restrictions and availability of company resources (both staff and equipment). Any weather hazards and conditions affecting the flight were continuously monitored due to their impact on the daily success of airborne and ground operations.

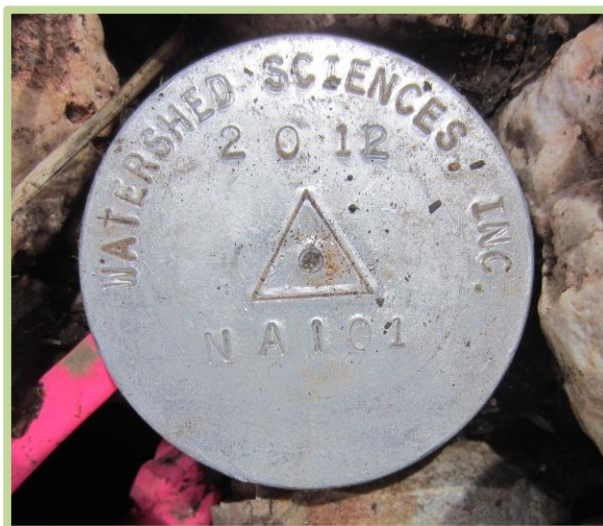
Ground Survey

Monumentation

The spatial configuration of ground survey monuments provided redundant control within 13 nautical miles of the mission area for LiDAR flights. Monuments were also used for collection of ground control points using RTK survey techniques (see section **RTK** below).

Monument locations were selected with consideration for satellite visibility, field crew safety, and optimal location for RTK coverage. WSI utilized three existing monuments and established 13 new monuments for the Kaibab National Forest project (Table 3, Figure 2). Existing monumentation included two US DOT highway monuments and one US Forest Service monument. All new monumentation other than NP_PK_01 was set using 5/8" rebar topped with stamped 2" aluminum caps. NP_PK_01 is a 6 inch unmarked surveyor's nail set in hard-packed soil for the sole purpose of RTK collection.

To correct the continuous onboard measurements of the aircraft position recorded throughout the missions, WSI concurrently conducted multiple static Global Navigation Satellite System (GNSS) ground surveys (1 Hz recording frequency) over each monument. After the airborne survey, the static GPS data were triangulated with nearby Continuously Operating Reference Stations (CORS) using the Online Positioning User Service (OPUS¹) for precise positioning. Multiple independent sessions over the same monument were processed to confirm antenna height measurements and to refine position accuracy.



Static surveys were collected using a combination of Trimble model R7 GNSS receivers equipped with a Zephyr Geodetic Model 2 RoHS antenna, Trimble model R6 (Model 2) GNSS receivers, and Trimble model R8 (Model 2) GNSS receivers. All GNSS measurements were made with dual frequency L1-L2 receivers with carrier-phase correction. See Table 4 for Trimble unit specifications.

¹ OPUS is a free service provided by the National Geodetic Survey to process corrected monument positions. <http://www.ngs.noaa.gov/OPUS>.

Table 3: Monuments established for the Kaibab National Forest acquisition. Coordinates are on the NAD83 (HARN) datum, epoch 2002

| Monument ID | Established By | Latitude | Longitude | Ellipsoid (meters) |
|-------------|----------------|-------------------|---------------------|--------------------|
| NAI_01 | WSI | 36° 33' 12.22211" | -112° 10' 33.63884" | 2675.432 |
| NAI_02 | WSI | 36° 26' 35.6385" | -112° 9' 43.40595" | 2773.118 |
| NAI_03 | WSI | 36° 35' 25.93281" | -112° 10' 45.30344" | 2639.897 |
| NAI_04 | WSI | 36° 24' 4.51954" | -112° 7' 49.83417" | 2634.509 |
| NAI_05 | WSI | 36° 46' 9.41694" | -112° 15' 16.65935" | 2288.202 |
| NAI_06 | WSI | 36° 45' 56.75056" | -112° 15' 52.54113" | 2302.459 |
| NAI_07 | WSI | 36° 40' 57.23646" | -112° 12' 55.74251" | 2458.558 |
| NAI_08 | WSI | 36° 23' 50.48325" | -112° 14' 27.14183" | 2579.041 |
| NAI_09 | WSI | 36° 26' 21.80473" | -112° 14' 28.30581" | 2524.606 |
| NAI_10 | WSI | 36° 18' 2.85829" | -111° 59' 59.32344" | 2678.255 |
| NAI_11 | WSI | 36° 18' 11.58665" | -111° 59' 41.62636" | 2669.985 |
| NAI_12 | WSI | 36° 37' 53.7857" | -112° 10' 24.81587" | 2583.394 |
| NP_PK_01* | WSI | 36° 13' 10.99251" | -111° 57' 17.09874" | 2558.308 |
| USDOT_01 | US DOT | 36° 21' 20.29061" | -112° 7' 7.05959" | 2654.158 |
| USDOT_02 | US DOT | 36° 20' 26.03216" | -112° 7' 1.84364" | 2659.633 |
| USFS_AZ_22 | USFS | 36° 30' 6.07827" | -112° 8' 18.47778" | 2588.292 |

*NP_PK_01 is an unmarked 6 inch surveyor's nail set in hard-packed soil for RTK collection.

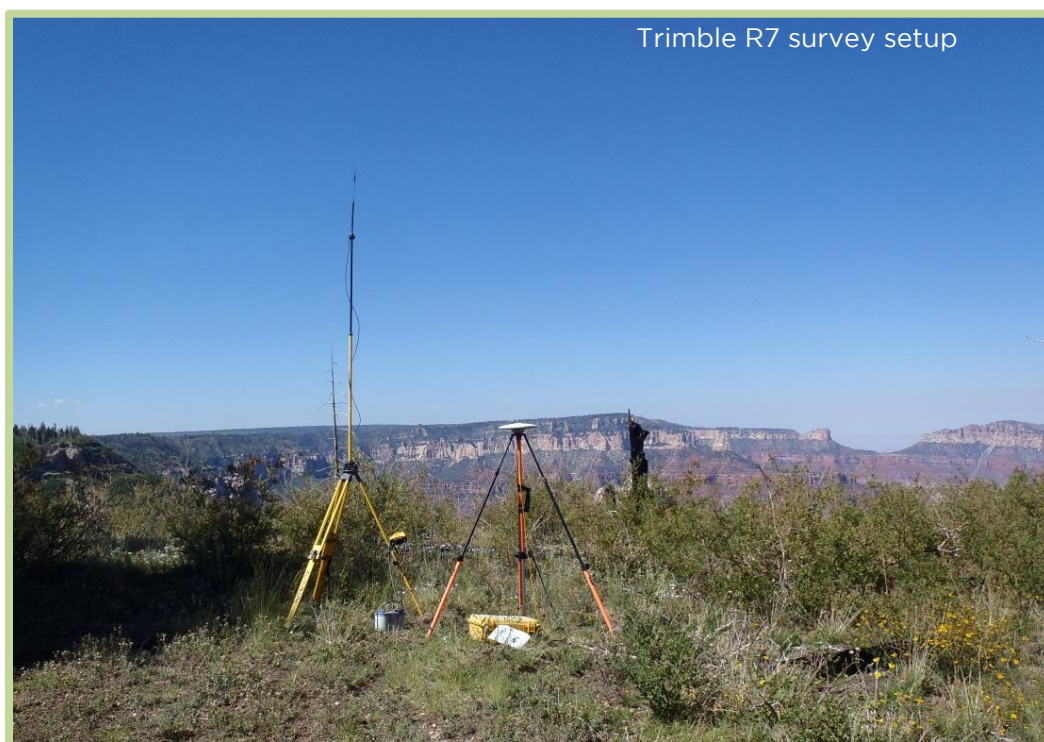
Table 4: Trimble equipment identification

| Receiver Model | Antenna | OPUS Antenna ID | Use |
|-----------------|-------------------------------|-----------------|-------------|
| Trimble R6 GNSS | Integrated Antenna R6 Model 2 | TRM_R6 | Static |
| Trimble R7 GNSS | Zephyr GNSS Geodetic Model 2 | TRM57971.00 | Static |
| Trimble R8 GNSS | Integrated Antenna R8 Model 2 | TRM_R8_GNSS | Static, RTK |

RTK

For the RTK check point data collection, a Trimble R7 base unit was positioned at a nearby monument to broadcast a kinematic correction to a roving Trimble R6 or R8 GNSS receiver. All RTK measurements were made during periods with a Position Dilution of Precision (PDOP) of ≤ 3.0 with at least six satellites in view of the stationary and roving receivers. When collecting RTK data, the rover would record data while stationary for five seconds, then calculate the pseudorange position using at least three one-second epochs. Relative errors for the position must be less than 1.5 cm horizontal and 2 cm vertical in order to be accepted.

RTK positions were collected on hard surface locations such as gravel or stable dirt roads that also had good satellite visibility. RTK measurements were not taken on highly reflective surfaces such as center line stripes or lane markings on roads. The distribution of RTK points depended on ground access constraints, and may not be equitably distributed throughout the study area. See Figure 2 to view the distribution of RTK in this project.



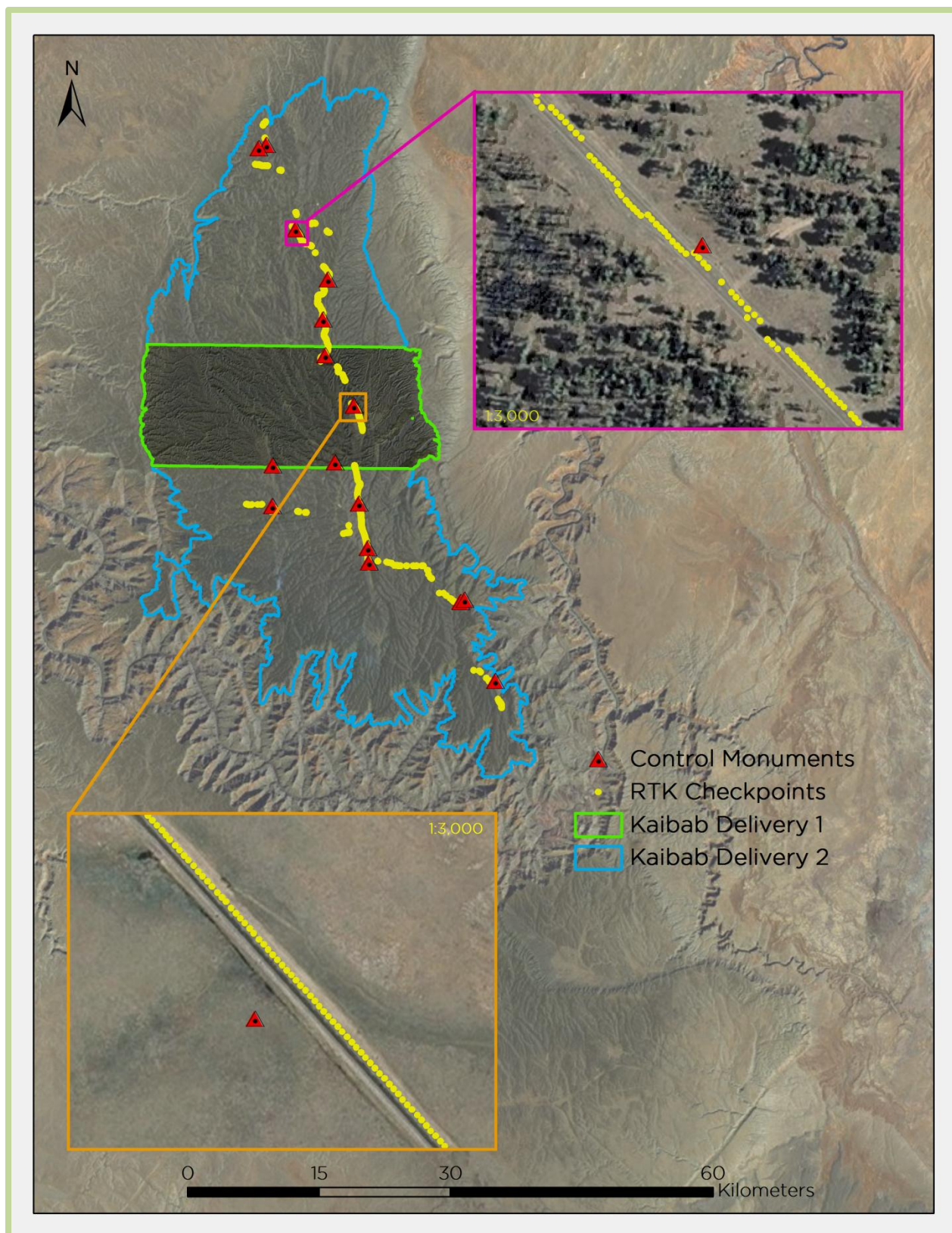


Figure 2: Basestation and RTK checkpoint location map

Airborne Survey

LiDAR

The LiDAR survey was accomplished with a Leica ALS50 Phase II and ALS60 system dually mounted in a Cessna Caravan. Table 5 summarizes the settings used to yield an average pulse density of ≥ 8 pulses/m² over the Kaibab National Forest terrain. It is not uncommon for some types of surfaces (e.g. dense vegetation or water) to return fewer pulses than the laser originally emitted. These discrepancies between native and delivered density will vary depending on terrain, land cover, and the prevalence of water bodies.

Table 5: LiDAR survey settings and specifications for the Kaibab National Forest site

| LiDAR Survey Settings & Specifications | | | |
|--|---------------------------------|---------------------------------|---|
| Survey Altitude (AGL) | 900 m | 1200 m | 2000 m |
| Target Pulse Rate | 106 kHz | 88 kHz | 50 kHz (SPiA) 100 kHz (MPiA) |
| Sensor Configuration | Single Pulse in Air (SPiA) | Single pulse in air (SPiA) | Single Pulse in Air (SPiA) Multi Pulse in Air (MPiA) |
| Laser Pulse Diameter | 21 cm | 28 cm | 45 cm |
| Mirror Scan Rate | 66.3 Hz | 50.3 Hz | 49.3 Hz (ALS50) 56 Hz (ALS 60) |
| Field of View | 26° | 28° | 20° |
| GPS Baselines | ≤ 13 nm | ≤ 13 nm | ≤ 13 nm |
| GPS PDOP | ≤ 3.2 | ≤ 3.2 | ≤ 3.2 |
| GPS Satellite Constellation | ≥ 6 | ≥ 6 | ≥ 6 |
| Maximum Returns | 4 | 4 | 4 |
| Intensity | 8-bit | 8-bit | 8-bit |
| Resolution/Density | Average 8 pulses/m ² | Average 8 pulses/m ² | Average 8 pulses/m ² |
| Accuracy | RMSE _z \leq 15 cm | RMSE _z \leq 15 cm | RMSE _z \leq 15 cm |

All areas were surveyed with an opposing flight line side-lap of $\geq 50\%$ ($\geq 100\%$ overlap) to reduce laser shadowing and increase surface laser painting. The Leica laser systems record up to four range measurements (returns) per pulse. All discernible laser returns were processed for the output dataset.

Due to the steepness of the terrain along the northern rim of Grand Canyon National Park, the angle of incidence is so extreme that some cliff edges and extreme drop offs were not able to be covered by the flight. Flight parameters were set to capture as much of the terrain as possible.

To accurately solve for laser point position (geographic coordinates x, y, z), the positional coordinates of the airborne sensor and the attitude of the aircraft were recorded continuously throughout the LiDAR data collection mission. Position of the aircraft was measured twice per second (2 Hz) by an onboard differential GPS unit. Aircraft attitude was measured 200 times per second (200 Hz) as pitch, roll, and yaw (heading) from an onboard inertial measurement unit (IMU). To allow for post-processing correction and calibration, aircraft/ sensor position and attitude data are indexed by GPS time.



3D point cloud looking up the southern canyon in the Kaibab National Forest



LiDAR Data

Post-acquisition, WSI processing staff initiated a suite of automated and manual techniques to process the data into the requested deliverables. Processing tasks included GPS control computations, kinematic corrections, calculation of laser point position, calibration for optimal relative and absolute accuracy, and classification of ground and non-ground points. Processing methodologies were tailored for the landscape and intended application of the point data (Table 6). A full description of these tasks can be found in Table 7.

Table 6: ASPRS LAS classification standards applied to the Kaibab National Forest dataset

| Classification Identification Number | Classification Name | Classification Description |
|--------------------------------------|-----------------------|--|
| 1 | Default/ Unclassified | Laser returns that are not included in the ground class and not dismissed as Noise or Withheld points. |
| 2 | Ground | Ground that is determined by a number of automated and manual cleaning algorithms to determine the best ground model the data can support. |
| 7 | Noise | Laser returns that are often associated with birds or artificial points below the ground surface “pits”. |
| 11 | Withheld | Laser returns that have intensity values of 0 or 255. |

Table 7: LiDAR processing workflow

| LiDAR Processing Step | Software Used |
|--|---|
| Resolve kinematic corrections for aircraft position data using kinematic aircraft GPS and static ground GPS data. | Waypoint GPS v.8.3 Trimble Business Center v.2.80 Blue Marble Desktop v.2.5 |
| Develop a smoothed best estimate of trajectory (SBET) file that blends post-processed aircraft position with attitude data. Sensor head position and attitude are calculated throughout the survey. The SBET data are used extensively for laser point processing. | IPAS TC v.3.1 |
| Calculate laser point position by associating SBET position to each laser point return time, scan angle, intensity, etc. Create raw laser point cloud data for the entire survey in *.las (ASPRS v. 1.2) format. Data are converted to orthometric elevations (NAVD88) by applying a Geoid03 correction. | ALS Post Processing Software v.2.74 |
| Import raw laser points into manageable blocks (less than 500 MB) to perform manual relative accuracy calibration and filter erroneous points. Ground points are then classified for individual flight lines (to be used for relative accuracy testing and calibration). | TerraScan v.12.004 |
| Using ground classified points per each flight line, the relative accuracy is tested. Automated line-to-line calibrations are then performed for system attitude parameters (pitch, roll, heading), mirror flex (scale) and GPS/IMU drift. Calibrations are performed on ground classified points from paired flight lines. Every flight line is used for relative accuracy calibration. | TerraMatch v.12.001 |
| Import position and attitude data. Classify resulting data as ground and non-ground points. Assess statistical absolute accuracy via direct comparisons of ground classified points to ground RTK survey data. | TerraScan v.12.004 TerraModeler v.12.002 |
| Generate bare earth models as triangulated surfaces, export as ArcInfo ASCII grids at 1 meter pixel resolution, and mosaic as ESRI grids. Also export ASCII grids of the first return point surface at 1 meter pixel resolution to generate highest hit models. | TerraScan v.12.004 ArcMap v. 10.0 TerraModeler v.12.002 |

Due to the extreme terrain at the southern end of the Kaibab National Forest, the angle of incidence created areas in the data where laser returns did not hit the ground. These areas were minimal and only occur on steep cliffs. In the few affected areas, the resulting ground model will show minimal stretching as the points are bridged across the gap to create a surface (Figure 3).

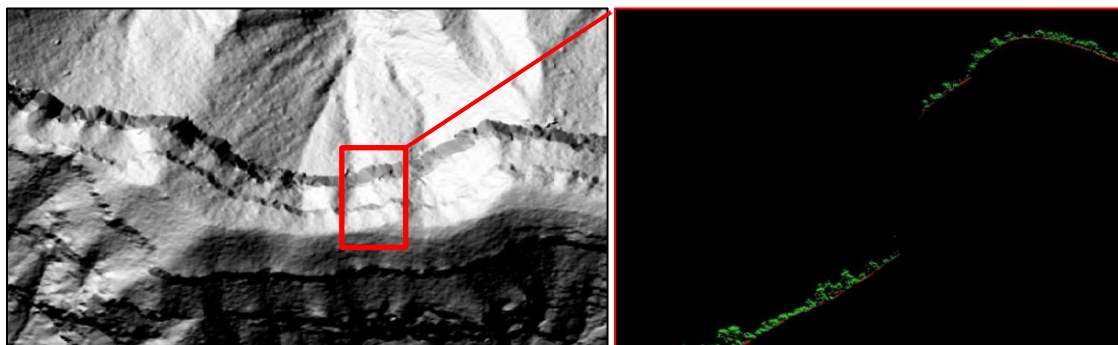


Figure 3: Bare earth model and laser returns over steep terrain in Kaibab National Forest.

3D point cloud looking over the southern side of the canyon in the Kaibab National Forest ►



LiDAR Density

The average first-return density for the complete LiDAR dataset was 9.97 points/m² (Table 8). The pulse density distribution will vary within the study area due to laser scan pattern and flight conditions. Additionally, some types of surfaces (i.e. breaks in terrain, water, steep slopes) may return fewer pulses (delivered density) than originally emitted by the laser (native density).

The statistical distribution of first returns (Figure 4) and classified ground points (Figure 5) are portrayed below. Also presented are the spatial distribution of average first return densities (Figure 6 and Figure 7) and ground point densities (Figure 8 and Figure 9) for each 100 m² cell. Statistics presented are for the entire LiDAR project area.

Table 8: Average LiDAR point densities

| Classification | Point Density |
|-------------------|----------------------------|
| First-Return | 9.97 points/m ² |
| Ground Classified | 4.25 points/m ² |

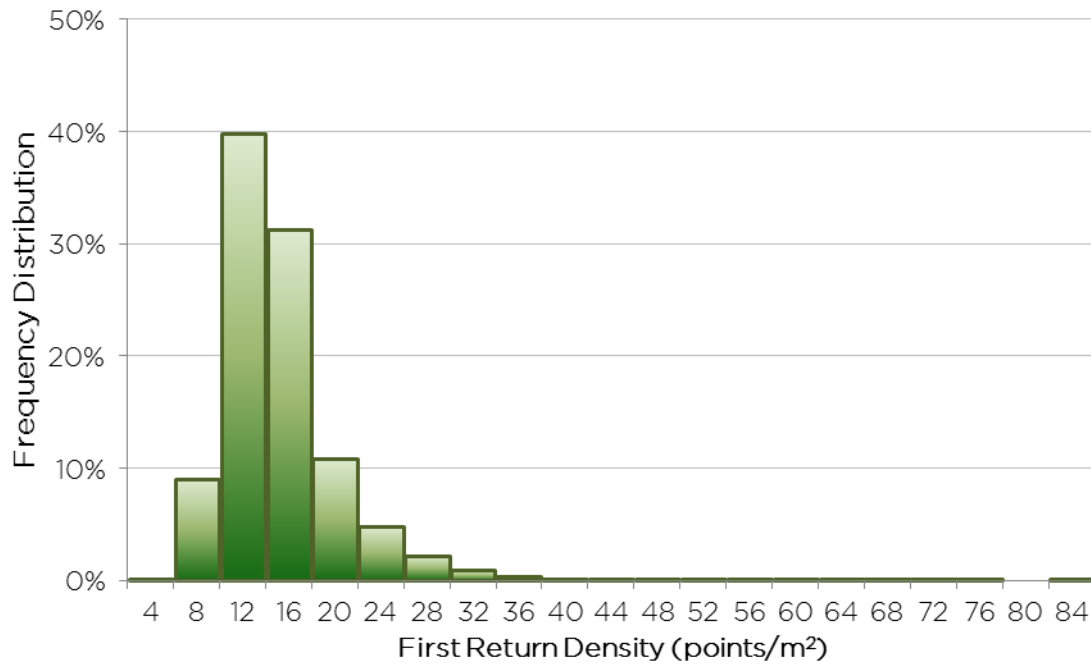


Figure 4: Frequency distribution of first return densities (native densities) of the 1m gridded study area

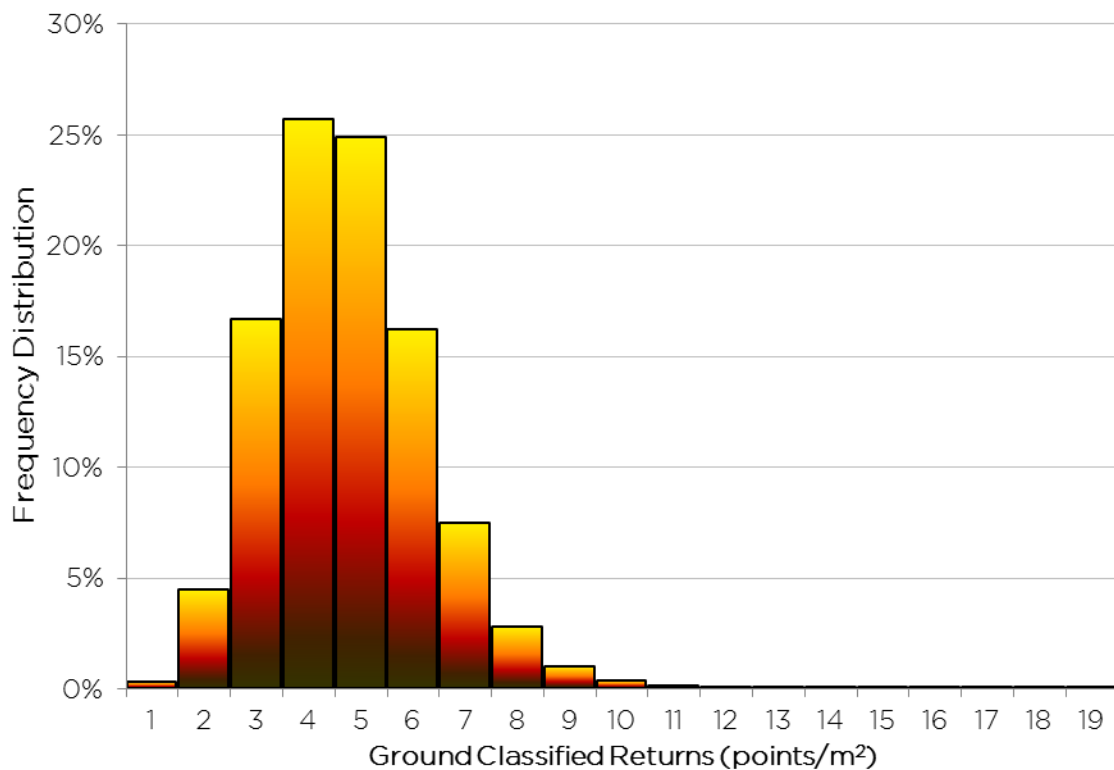


Figure 5: Frequency distribution of ground return densities of the 1m gridded study area

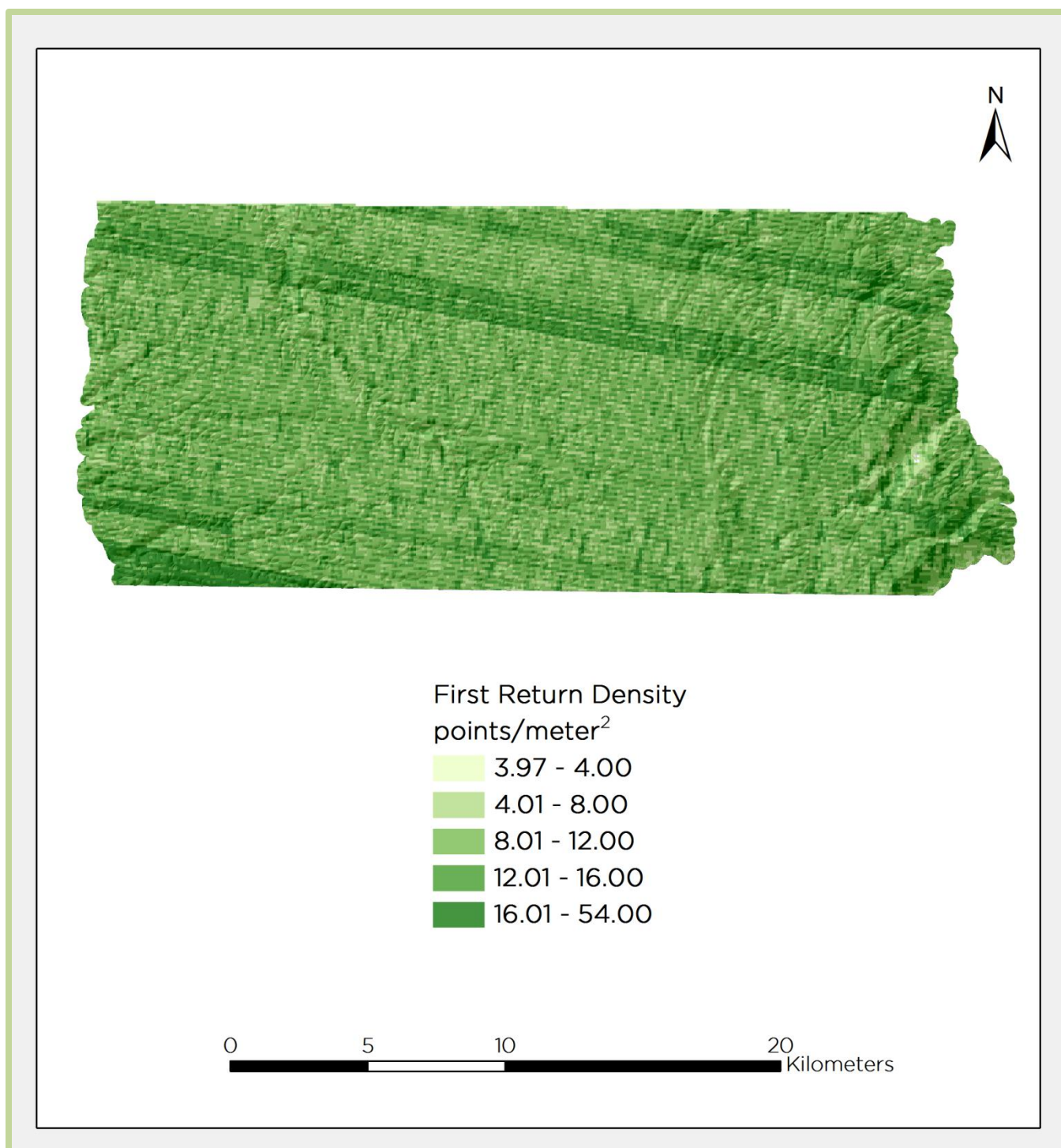


Figure 6: Delivery 1 native density map for the Kaibab National Forest site

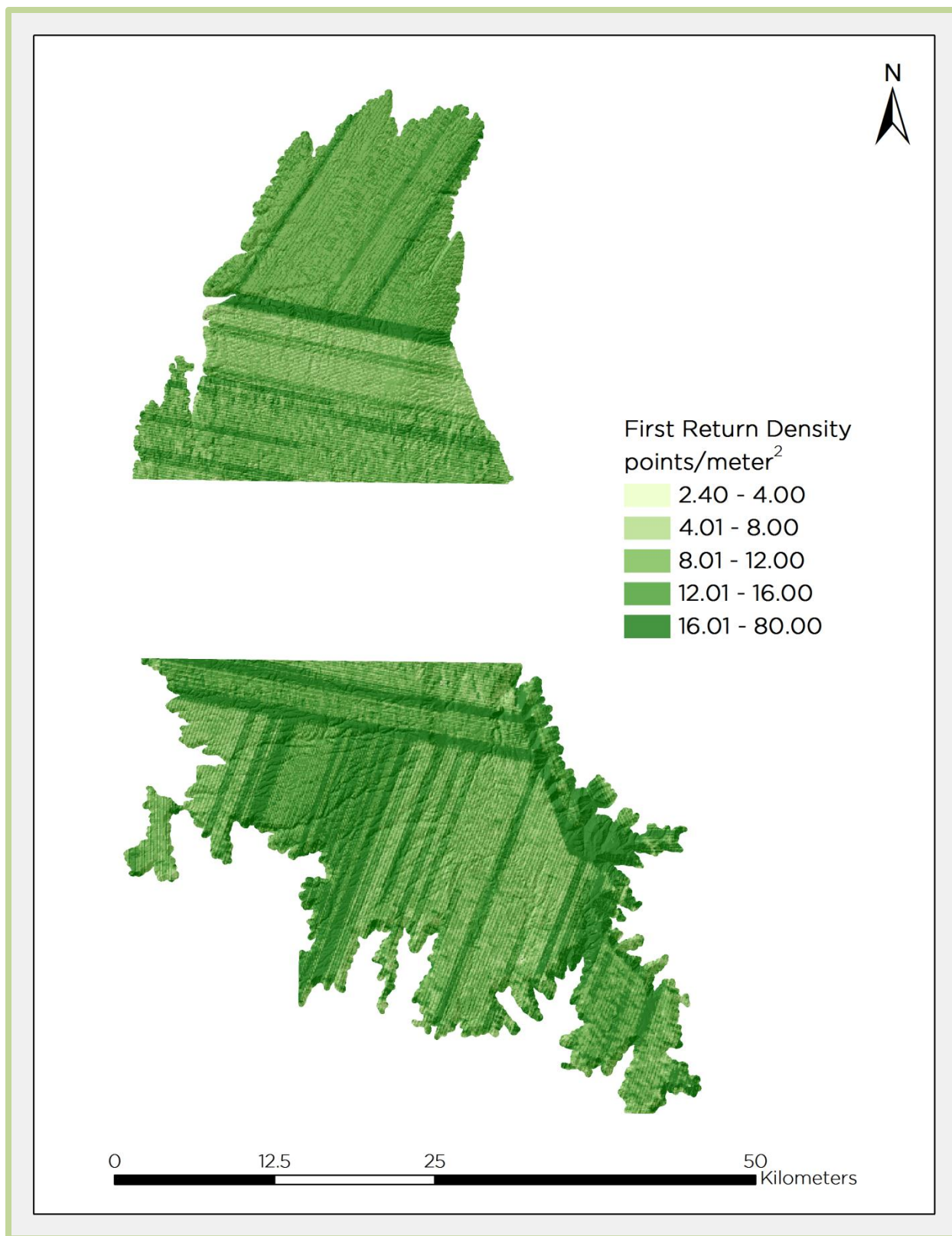


Figure 7: Delivery 2 native density map for the Kaibab National Forest site

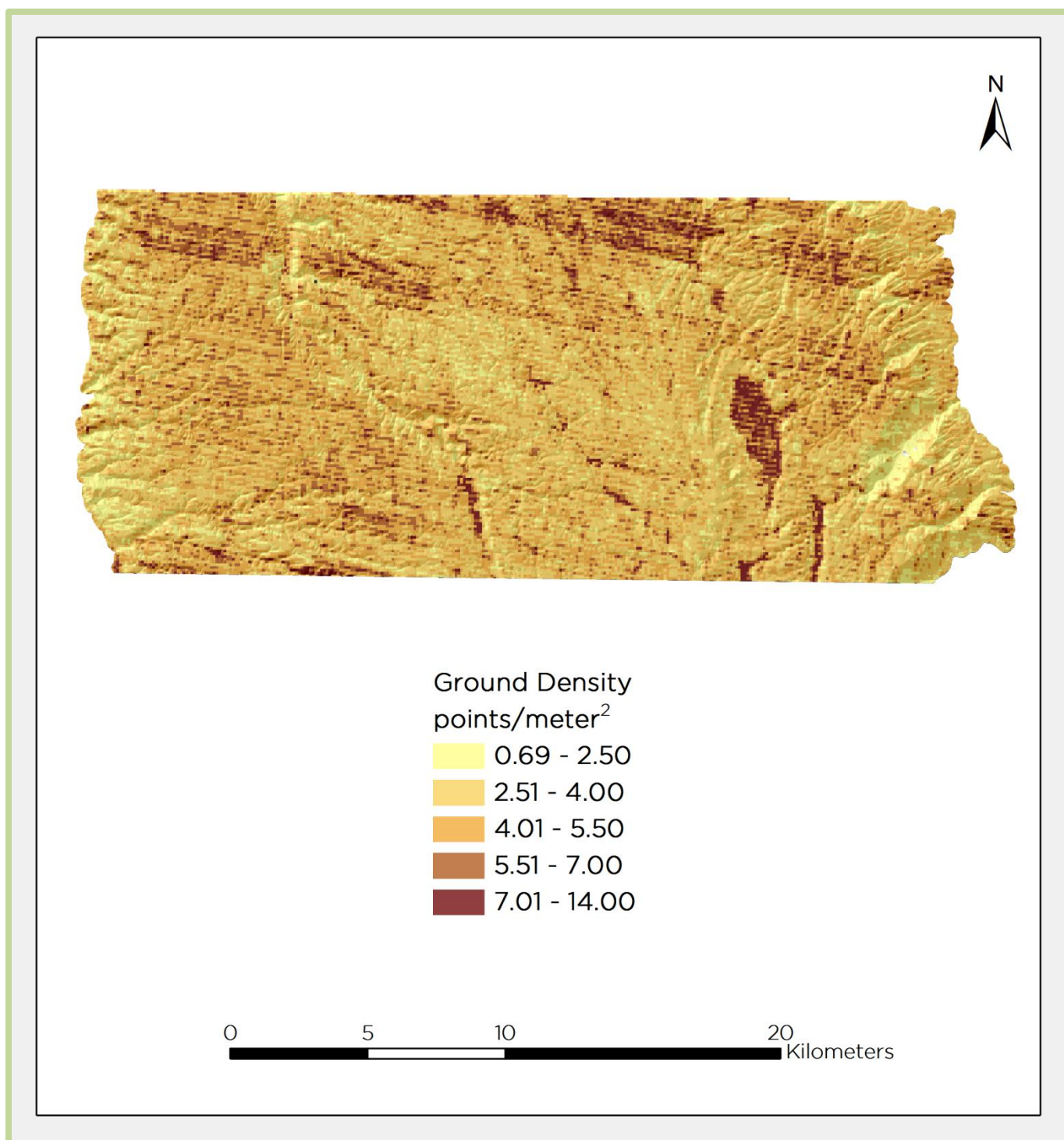


Figure 8: Delivery 1 ground density map for the Kaibab National Forest site

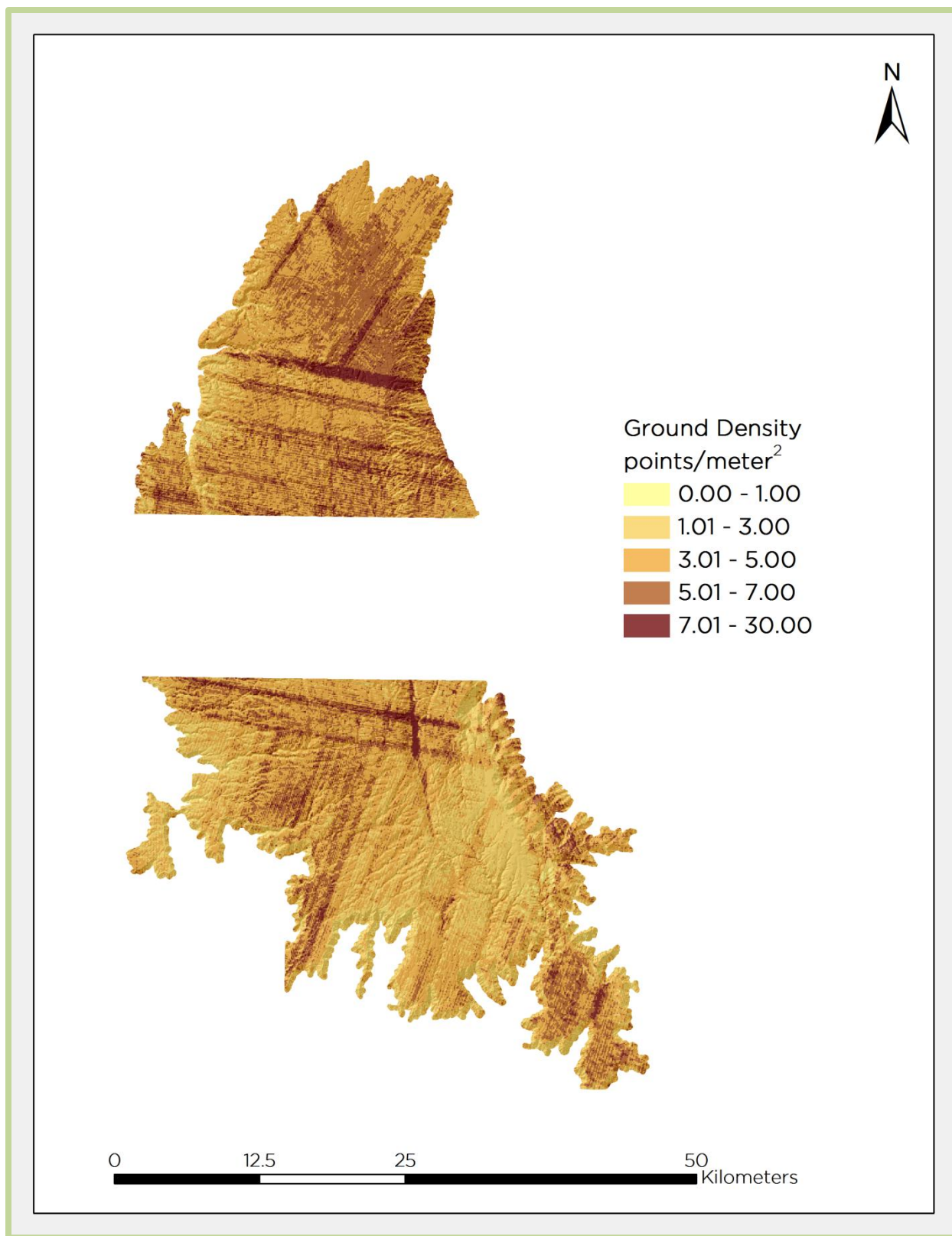


Figure 9: Delivery 2 ground density map for the Kaibab National Forest site

LiDAR Accuracy Assessments

The accuracy of the LiDAR data collection can be described as the consistency of the data with external data sources (absolute accuracy) and the consistency of the dataset with itself (relative accuracy). See Appendix A for further information on sources of error.

LiDAR Absolute Accuracy

Vertical absolute accuracy was primarily assessed from ground check point data collected on open, bare earth surfaces with level slope ($<20^\circ$). Fundamental Vertical Accuracy (FVA) reporting is designed to meet guidelines presented in the National Standard for Spatial Data Accuracy (FGDC, 1998). FVA compares known RTK ground survey check points to the triangulated ground surface generated by the LiDAR points. FVA is a measure of the accuracy of LiDAR point data in open areas where the LiDAR system has a “very high probability” of measuring the ground surface and is evaluated at the 95% confidence interval (1.96σ).

Absolute accuracy is described as the mean and standard deviation (σ) of divergence of the ground surface model from ground survey point coordinates. These statistics assume the error for x, y, and z is normally distributed, and therefore the skew and kurtosis of distributions are also considered when evaluating error statistics. For the Kaibab National Forest LiDAR survey, 7,448 hard surface RTK points were collected in total.

Table 9: Absolute and relative accuracies

| | Absolute Accuracy | Relative Accuracy |
|------------|-------------------|-------------------|
| Sample | 7448 points | 1622 surfaces |
| Average | -0.005 m | 0.045 m |
| Median | -0.004 m | 0.045 m |
| RMSE | 0.030 m | 0.051 m |
| 1 σ | 0.030 m | 0.019 m |
| 2 σ | 0.059 m | 0.036 m |

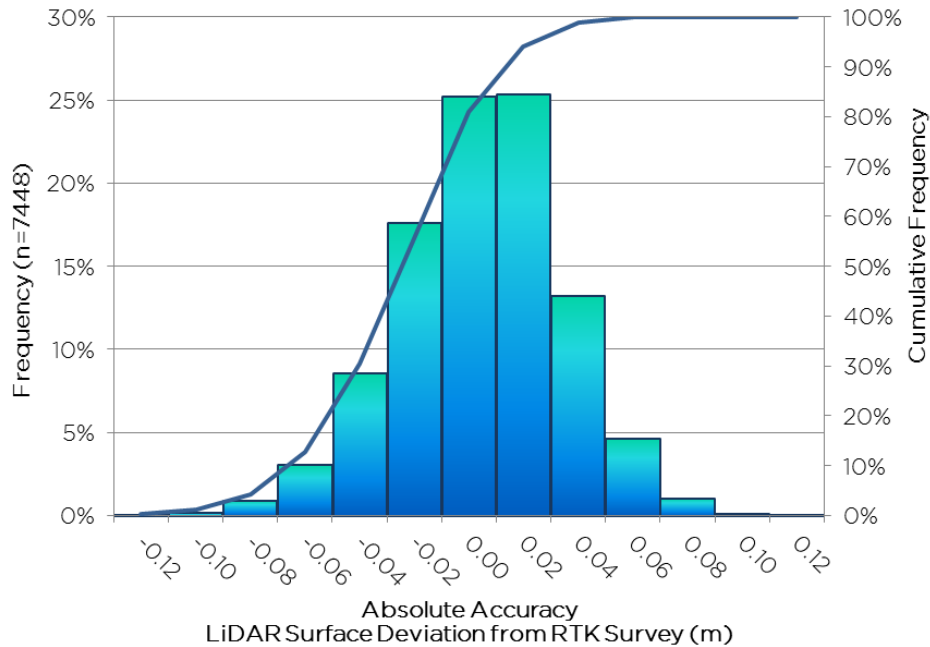


Figure 10: Frequency histogram for LiDAR surface deviation from RTK values

LiDAR Relative Accuracy

Relative accuracy refers to the internal consistency of the data set as a whole—that is, the ability to place an object in the same location given multiple flight lines, GPS conditions, and aircraft attitudes. The relative accuracy is computed by comparing the ground surface model of each individual flight line with its neighbors in overlapping regions (Figure 11). When the LiDAR system is well calibrated, the swath-to-swath divergence is low (<10cm). See Appendix B for operational measures taken to improve relative accuracy.

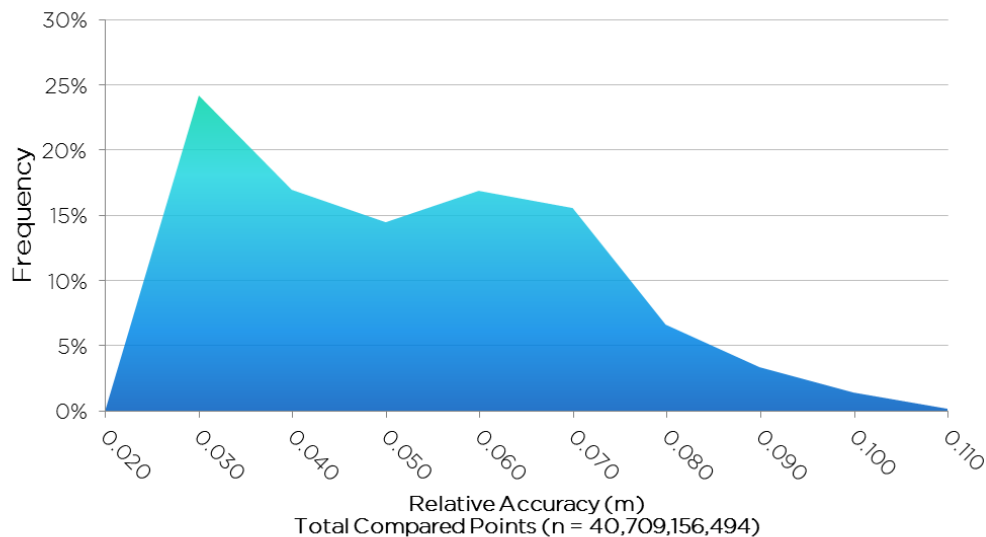


Figure 11: Frequency plot for relative accuracy between flight lines



Figure 12: View looking west at Cape Final of the Walhalla Plateau in Kaibab National Forest, AZ. Image derived from gridded LiDAR points colored by 2010 NAIP imagery.



Figure 13: View looking north up a canyon of the Walhalla Plateau in Kaibab National Forest, AZ. Image derived from LiDAR point cloud colored by 2010 NAIP imagery.

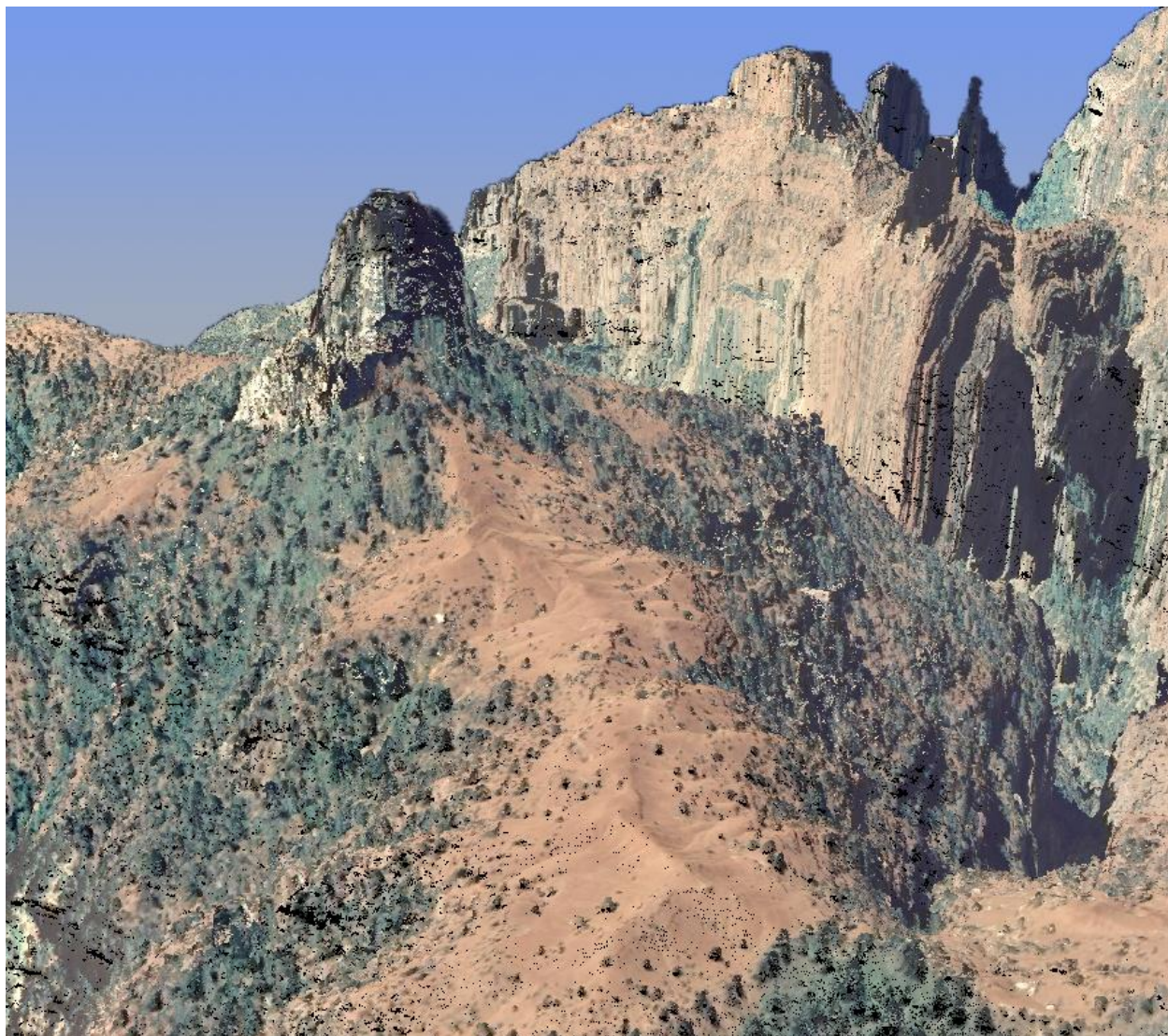


Figure 14: View looking south at Mount Hayden and Hancock Butte in Kaibab National Forest, AZ. Image derived from LiDAR point cloud colored by 2010 NAIP imagery.

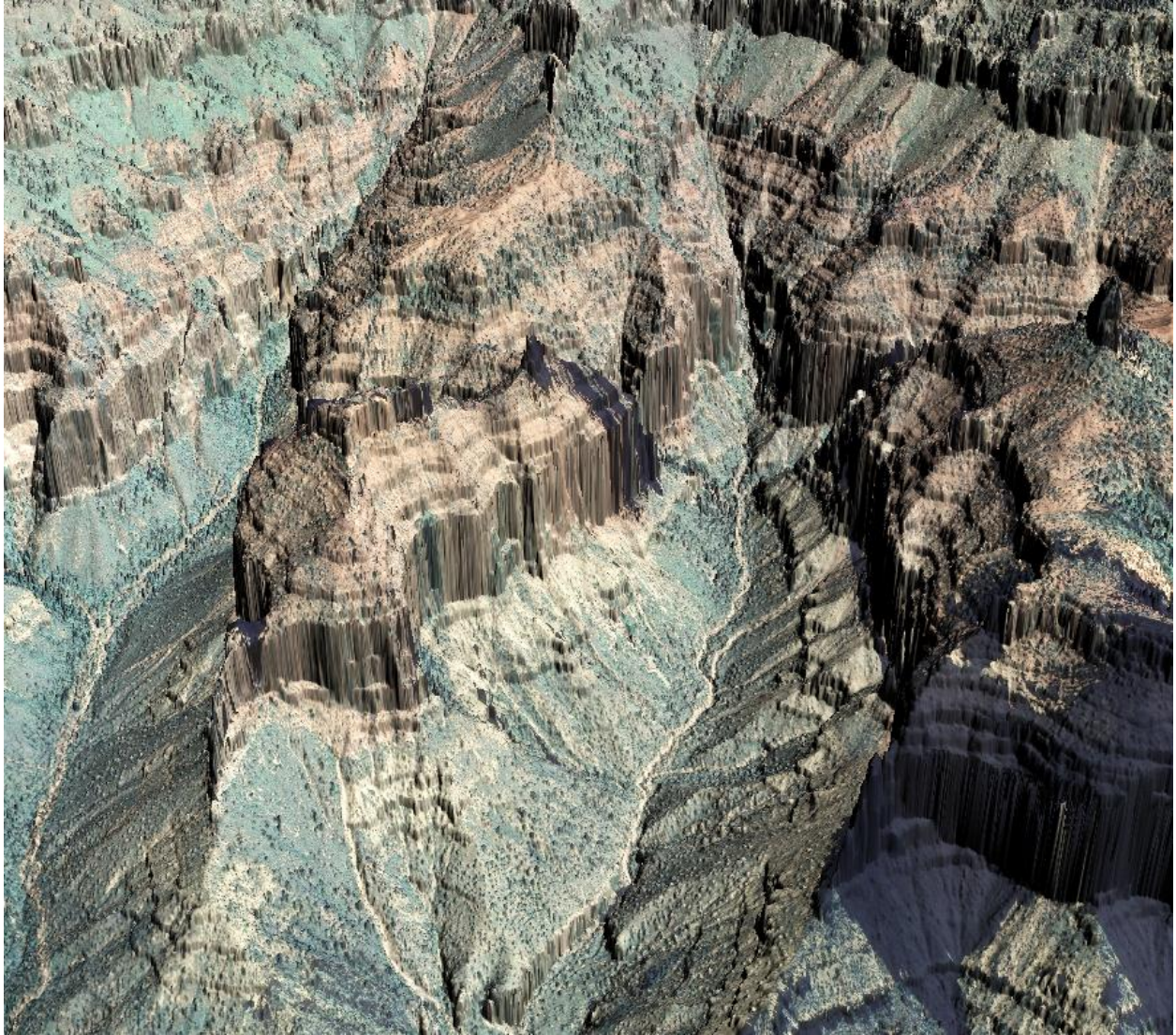


Figure 15: View looking north into Nankoweap Canyon. Image derived from gridded LiDAR points colored by 2010 NAIP imagery.

GLOSSARY

1-sigma (σ) Absolute Deviation: Value for which the data are within one standard deviation (approximately 68th percentile) of a normally distributed data set.

1.96-sigma (σ) Absolute Deviation: Value for which the data are within two standard deviations (approximately 95th percentile) of a normally distributed data set.

Root Mean Square Error (RMSE): A statistic used to approximate the difference between real-world points and the LiDAR points. It is calculated by squaring all the values, then taking the average of the squares and taking the square root of the average.

Pulse Rate (PR): The rate at which laser pulses are emitted from the sensor; typically measured as thousands of pulses per second (kHz).

Pulse Returns: For every laser pulse emitted, the Leica ALS 60 system can record *up to four* wave forms reflected back to the sensor. Portions of the wave form that return earliest are the highest element in multi-tiered surfaces such as vegetation. Portions of the wave form that return last are the lowest element in multi-tiered surfaces.

Accuracy: The statistical comparison between known (surveyed) points and laser points. Typically measured as the standard deviation (σ) and root mean square error (RMSE).

Intensity Values: The peak power ratio of the laser return to the emitted laser. It is a function of surface reflectivity.

Data Density: A common measure of LiDAR resolution, measured as points per square meter.

Spot Spacing: Also a measure of LiDAR resolution, measured as the average distance between laser points.

Nadir: A single point or locus of points on the surface of the earth directly below a sensor as it progresses along its flight line.

Scan Angle: The angle from nadir to the edge of the scan, measured in degrees. Laser point accuracy typically decreases as scan angles increase.

Overlap: The area shared between flight lines, typically measured in percents; 100% overlap is essential to ensure complete coverage and reduce laser shadows.

DTM / DEM: These often-interchanged terms refer to models made from laser points. The digital elevation model (DEM) refers to all surfaces, including bare ground and vegetation, while the digital terrain model (DTM) refers only to those points classified as ground.

Real-Time Kinematic (RTK) Survey: GPS surveying is conducted with a GPS base station deployed over a known monument with a radio connection to a GPS rover. Both the base station and rover receive differential GPS data and the baseline correction is solved between the two. This type of ground survey is accurate to 1.5 cm or less.

Laser Noise

For any given target, laser noise is the breadth of the data cloud per laser return (i.e., last, first, etc.). Lower intensity surfaces (roads, rooftops, still/calm water) experience higher laser noise. The laser noise range for this survey was approximately 0.02 meters.

Relative Accuracy

Relative accuracy refers to the internal consistency of the data set - the ability to place a laser point in the same location over multiple flight lines, GPS conditions, and aircraft attitudes. Affected by system attitude offsets, scale, and GPS/IMU drift, internal consistency is measured as the divergence between points from different flight lines within an overlapping area. Divergence is most apparent when flight lines are opposing. When the LiDAR system is well calibrated, the line-to-line divergence is low (<10 cm).

Relative Accuracy Calibration Methodology

Manual System Calibration: Calibration procedures for each mission require solving geometric relationships that relate measured swath-to-swath deviations to misalignments of system attitude parameters. Corrected scale, pitch, roll and heading offsets were calculated and applied to resolve misalignments. The raw divergence between lines was computed after the manual calibration was completed and reported for each survey area.

Automated Attitude Calibration: All data were tested and calibrated using TerraMatch automated sampling routines. Ground points were classified for each individual flight line and used for line-to-line testing. System misalignment offsets (pitch, roll and heading) and scale were solved for each individual mission and applied to respective mission datasets. The data from each mission were then blended when imported together to form the entire area of interest.

Automated Z Calibration: Ground points per line were used to calculate the vertical divergence between lines caused by vertical GPS drift. Automated Z calibration was the final step employed for relative accuracy calibration.

Absolute Accuracy

The vertical accuracy of LiDAR data is described as the mean and standard deviation (σ) of divergence of LiDAR point coordinates from RTK ground survey point coordinates. To provide a sense of the model predictive power of the dataset, the root mean square error (RMSE) for vertical accuracy is also provided. These statistics assume the error distributions for x, y, and z are normally distributed, thus we also consider the skew and kurtosis of distributions when evaluating error statistics.

LiDAR accuracy error sources and solutions:

| Type of Error | Source | Post Processing Solution |
|---------------------------|------------------------------|---|
| GPS (Static/Kinematic) | Long Base Lines | None |
| | Poor Satellite Constellation | None |
| | Poor Antenna Visibility | Reduce Visibility Mask |
| Relative Accuracy | Poor System Calibration | Recalibrate IMU and sensor offsets/settings |
| | Inaccurate System | None |
| Laser Noise | Poor Laser Timing | None |
| | Poor Laser Reception | None |
| | Poor Laser Power | None |
| | Irregular Laser Shape | None |

Operational measures taken to improve relative accuracy:

Low Flight Altitude: Terrain following is employed to maintain a constant above ground level (AGL). Laser horizontal errors are a function of flight altitude above ground (i.e., $\sim 1/3000^{\text{th}}$ AGL flight altitude).

Focus Laser Power at narrow beam footprint: A laser return must be received by the system above a power threshold to accurately record a measurement. The strength of the laser return is a function of laser emission power, laser footprint, flight altitude and the reflectivity of the target. While surface reflectivity cannot be controlled, laser power can be increased and low flight altitudes can be maintained.

Reduced Scan Angle: Edge-of-scan data can become inaccurate. The scan angle was reduced to a maximum of 315° from nadir, creating a narrow swath width and greatly reducing laser shadows from trees and buildings.

Quality GPS: Flights took place during optimal GPS conditions (e.g., 6 or more satellites and PDOP [Position Dilution of Precision] less than 3.0). Before each flight, the PDOP was determined for the survey day. During all flight times, a dual frequency DGPS base station recording at 1-second epochs was utilized and a maximum baseline length between the aircraft and the control points was less than 19 km (11.5 miles) at all times.

Ground Survey: Ground survey point accuracy (i.e. <1.5 cm RMSE) occurs during optimal PDOP ranges and targets a minimal baseline distance of 4 miles between GPS rover and base. Robust statistics are, in part, a function of sample size (n) and distribution. Ground survey RTK points are distributed to the extent possible throughout multiple flight lines and across the survey area.

50% Side-Lap (100% Overlap): Overlapping areas are optimized for relative accuracy testing. Laser shadowing is minimized to help increase target acquisition from multiple scan angles. Ideally, with a 50% side-lap, the most nadir portion of one flight line coincides with the edge (least nadir) portion of overlapping flight lines. A minimum of 50% side-lap with terrain-followed acquisition prevents data gaps.

Opposing Flight Lines: All overlapping flight lines are opposing. Pitch, roll and heading errors are amplified by a factor of two relative to the adjacent flight line(s), making misalignments easier to detect and resolve.